Defect states in plastically deformed *n*-type silicon

D. Cavalcoli and A. Cavallini
INFM-Bologna and Department of Physics, University of Bologna, viale Berti Pichat 6/II, I-40127 Bologna, Italy

E. Gombia
CNR MASPEC Institute, via Chiavari 18/A, I-43100 Parma, Italy

(Received 4 January 1996; revised manuscript received 28 February 1997)

The electronic properties of deformed *n*-type silicon have been investigated via deep-level transient spectroscopy (DLTS). The four deformation-induced levels usually labeled in the literature as *A*, *B*, *C*, and *D* have been found. Their analysis as a function of the deformation parameters and the study of their thermal stability have allowed us to conclude that only the *C* line, located 0.40 eV from the conduction-band edge, can be attributed to dislocations. The characteristics of this line are reported and discussed, taking advantage of the fact that, owing to the deformation conditions employed, it could be clearly resolved and analyzed in the spectra. The DLTS peaks have been simulated by the introduction of a broadening parameter, whose dependence on the dislocation density has been studied. Moreover, the capture kinetic of this line has been analyzed. The broadening of the observed DLTS peaks has been analyzed on the basis of two different physical mechanisms: crystal disorder and inhomogeneities in the Coulomb potential along the dislocation lines. A tentative identification of the defects responsible for the deep levels observed has been given. [S0163-1829(97)07840-5]

10.1103/PhysRevB.56.10208

I. INTRODUCTION

The electronic properties of extended defects have been studied for many years by several groups.[1] This subject has gained particular interest in recent years as dislocation-induced states increase the quantum efficiency of luminescence in silicon and light emission from silicon-based devices has recently attracted considerable attention.[2] Nevertheless, the question which energy levels in the band gap are due to dislocations is far to be understood as plastic deformation introduces a large amount of point defects in the crystal in addition to dislocations. Since the investigated electrical properties are mainly due to point defect effects, it is often difficult to separate the point defect from the extended defect contributions.

Moreover, deep-level transient spectroscopy (DLTS) needs careful analysis when applied to plastically deformed silicon since several problems must be considered.

(i) Dislocations are extended defects and consequently they can change their charge state within wide limits. The Coulomb interaction among charges confined at the dislocation causes a shift of the dislocation level with respect to the Fermi level: This local band bending induces a change in the positions of the energy levels during filling and emptying of the traps.

(ii) The presence of the Coulomb potential around the dislocation has also been considered as the reason for the ''logarithmic filling time behavior'' of extended defects.[1]

(iii) Due to the dislocation strain field the capacitance transients are often nonexponential,[1] which gives broadened DLTS peaks. This effect can result in either symmetrically[3] or asymmetrically[4,5] broadened lines. The first ones can be ascribed to the effect of the deformation-induced disorder on the energy levels and the second ones can be explained only by taking into account the electron equilibration at the defect, as modeled by the authors of Ref. 5.

(iv) Sometimes the DLTS line amplitude shows an anomalous variation of the peak amplitude as a function of temperature and this feature has been ascribed to the amphoteric behavior of dislocation-related deep levels.[6]

Despite these difficulties, extensive work on plastically deformed *n*-type Si have led to the identification of four traps, labeled *A*, *B*, *C*, and *D*,[3] whose corresponding DLTS peaks are strongly dependent on deformation and annealing procedures.

The goal of this paper is the study of the main features regarding the *C* line. In fact, due to the deformation procedures used, this line dominates all the spectra and it could be clearly resolved and studied. We shall conclude that only the *C* line is closely related to dislocations.

First we will report the experimental evidence for ascribing the *C* line to the dislocations. Then the main characteristics of the *C* line, such as its thermal stability, its logarithmic capture law, and its symmetrical broadening, will be discussed. In conclusion, we hypothize the nature of the traps responsible for the observed levels.

II. MATERIALS

High-purity, float-zone, *n*-type, {111} Si single crystals, grown by Wacker Chemitronic, were used in this study. The doping level N_d-N_a was equal to 5×10^{13} (phosphorus atoms)/cm^3. Sample bars of 5×20 mm^2, with the longest edge along the [110] axis, were plastically deformed by creep (four-point bending) along the [112] direction in a reducing atmosphere of forming gas (92% N_2 and 8% H_2) using a quartz and nuclear graphite deformation apparatus. The plastic strain ranges from 1% to 1.5%. The deformation temperature T_d is equal to 650 °C and 750 °C, the deformation duration t_d to 60 and 24 h and the resolved shear stress τ to 38 and 25 MPa for the sets DAT1 and DAT3, respectively. The load has been removed after deformation before cooling

the sample to room temperature (the cooling rate was about 4 °C/min); therefore, a partial annealing must be allowed especially for the samples deformed at the highest temperature ($T_d = 750$ °C, set DAT3), so that a relaxation of the defect structure could possibly occur. In the DAT1 samples the dislocation density N_D ranges from 10^3 to 10^7 cm^{-2}, while in DAT3 it is from 10^3 to 10^8 cm^{-2}. From each deformed bar, a set of samples has been obtained: Each of them, 5×2 mm^2 with the longest side along the [112] direction, has a nearly uniform dislocation density. Some of these samples were annealed at 850 °C for 1 h in forming gas (92% N_2 and 8% H_2). The most dislocated samples of each set before and after the annealing procedure were analyzed by high-voltage electron microscopy (HVEM).

After the treatments Schottky diodes (Au dots 1 mm in diameter) were prepared on the samples (2×5 mm^2 wide), while Ohmic contacts were realized with a Ga-Al alloy on the back surface. The diodes have been tested by current-voltage (I-V) plots to evaluate the series resistance and by capacitance-voltage (C-V) to obtain the effective free-carrier concentration. Hall effect and thermoelectric power measurements have been performed to check for compensation effects. After the samples were analyzed by DLTS. After removal of the diodes, the samples were annealed and Schottky diodes realized again in the previous position for DLTS measurements. This procedure has been necessary to overcome problems due to the inhomogeneous dislocation distribution, especially in the set DAT1.

III. METHODS

A. HVEM analyses

HVEM analyses were carried out in a JEM 1000 Electron Microscope (accelerating voltage 1 MV). To perform a structural characterization of the dislocations induced by deformation, the samples were thinned chemically by HNO_3/HF solutions and subsequently by ion milling up to 1 μm. Similarly prepared, reference samples heated at the same temperatures of DAT1 and DAT3, but not deformed, showed no evidence of dislocations. Moreover, in none of the deformed samples have precipitates been found.

In samples deformed at different temperatures some differences in the dislocation morphology were found by HVEM investigations. In DAT1 samples the dislocations are straight lines lying essentially along the glide bands, oriented along the [110] directions; most of them are 60° dissociated dislocations. Their distribution is strongly inhomogeneous and many intersections between dislocations are present. The dislocation distribution becomes homogeneous in DAT3 samples, where a preferential direction for the dislocation lines is still present. Here the dislocations are still straight lines, but with a lower number of intersections between them with respect to the previous case. No differences in the morphology or characteristics of dislocations between annealed and as-deformed samples were observed by HVEM analyses.

The dislocation density N_D evaluated by HVEM has been compared with the etch-pit density $N_{\rm ep}$. In the range of high N_D values (about 10^7 cm^{-2}), where the HVEM analysis could be performed, we found that $N_{\rm ep}$ underestimates N_D by a factor of about 2.

B. DLTS analyses

DLTS analyses were performed by a lock-in–type spectrometer of high sensitivity. Reverse bias $U_r = -7$ V and filling pulses $U_p = -0.3$ V have been used for most of the temperature scans presented here. Taking into account the doping density (5×10^{13} cm^{-3}) and the minimum capacitance variation measurable in our DLTS apparatus, the defect detectability limit relevant to our samples is about $(1-2) \times 10^{10}$ traps/cm^3.[7] Notwithstanding this low doping density, the weak-deformation procedure used allowed to avoid compensation effects. However, the choice of a lightly doped material gives high values of the series resistance of the diodes. Therefore, the measured capacitance variations have been corrected for the series resistance effects.[8]

The experimental capacitance transients relative to extended defects are, for nontrivial reasons, nonexponential, giving broadened DLTS peaks. Line broadening is a consequence of the spreading of defects states over an energy range. Symmetrical line broadening is successfully simulated by the introduction of a Gaussian distribution of activation enthalpies $G(E)$ centered around a mean value E_a, with standard deviation δ.[3] The capacitance transients of extended defects become

$$C(t) = C(0) \int_{-\infty}^{\infty} G(E) \exp[-e_n(E)t]\, dE, \qquad (1)$$

where $C(0)$ is the capacitance value at $t = 0$ and e_n represents the emission rate given by

$$e_n(E_a) = \sigma_n g \, \exp(\Delta S/k) \langle v_{\rm th} \rangle N_{\rm CB} \exp\left(\frac{E_a}{kT}\right), \qquad (2)$$

with σ_n the capture cross section, g the degeneracy factor, ΔS the ionization entropy, k the Boltzmann constant, $\langle v_{\rm th} \rangle$ the mean thermal velocity of majority carriers, $N_{\rm CB}$ the density of states in the conduction band, and T the absolute temperature. The parameters of each DLTS line to be fitted using this model are the prefactor $A_{\rm pf} = N_{\rm CB} \langle v_{\rm th} \rangle \sigma_n g \, \exp(\Delta S)/k$, the mean activation enthalpy E_a, the full width at half maximum (FWHM) of the Gaussian enthalpy distribution $\delta\sqrt{2 \ln 2}$, and $C(0)$. As all the parameters of each single DLTS line are highly correlated, at least two spectra taken at different frequencies must be fitted simultaneously.

IV. RESULTS

First it was checked that as-grown and reference samples did not show detectable DLTS peaks, meaning that the deep-level concentration in reference samples is lower than $(1-2) \times 10^{10}$ cm^{-3}. In all the deformed samples four DLTS levels with activation enthalpies $E_a = 0.19$, 0.29, 0.40, and 0.56 eV have been found. Their characteristic parameters are reported in Table I and the thermal emission rates e_n (T^2 corrected) are plotted versus the inverse temperature in the Arrhenius plot of Fig. 1, with data also from the literature.[1] Although the data scatter, it is clear that plastic deformation produces the same group of deep energy levels in different materials. These energy levels have been labeled A, B, C, and D, respectively,[3] and the same notation will be used

TABLE I. Results of DLTS investigations on a sample of the set DAT3 ($N_D \approx 10^4$ cm^{-2}) and a sample of the set DAT1 ($N_D \approx 10^6$ cm^{-2}). E_a represents the activation enthalpy, FWHM the full width at half maximum of the Gaussian enthalpy distribution, and A_{pf} the prefactor defined as $A_{pf} = \sigma_n \langle v_{th} \rangle N_{CB} g \exp(\Delta S/k)$, where $\langle v_{th} \rangle$ and N_{CB} are the thermal velocity and density of states in the conduction band, respectively, σ_n is the majority carrier capture cross section, g is the degeneracy factor, and ΔS is the change in entropy due to the emission of one electron from the deep level to the conduction band.

Set	Trap	E_a[a] (eV)	E_a[b] (eV)	FWHM (meV)	A_{pf}[a] (s^{-1})	A_{pf}[b] (s^{-1})	σ_n[c] (cm^2)
DAT3	*A*	0.19	0.23	0	6×10^6	3×10^9	
	B	0.29			2×10^7		
	C	0.40	0.43	44	5×10^6	1.3×10^8	8.9×10^{-16}
	D	0.56			2×10^7		
DAT1	*C*1	0.37	0.37	0	9.3×10^5	8.1×10^5	
	*C*2	0.43	0.43	0	1.2×10^6	4.0×10^7	
	C	0.42	0.39	13	2.6×10^7	2.2×10^7	8.3×10^{-16}

[a]Obtained from the Arrhenius plot e_n/T^2 vs $1/T$.
[b]Obtained from DLTS fitting (Omling model).
[c]Obtained from direct filling measurements.

from now on. The relative amplitudes of the $A-D$ lines change with dislocation density N_D, in particular for low N_D the lines are usually clearly resolved and not overlapped, while for high N_D some of them are usually more populated and mask the neighbor lines. The data in Fig. 1 refer to a sample deformed at 750 °C (of set DAT3) with low dislocation density ($N_D = 10^4$ cm^{-2}) where all the levels are clearly resolved.

Among these deformation-induced levels we believe that the *C* line is related to dislocations most closely for the following reasons.

(i) Figure 2(a) shows the trap concentration N_T in two samples of the set DAT3 ($N_D = 10^4$ cm^{-2}) before and after annealing. The contributions of *B* and *D* lines almost completely vanish after annealing. Therefore, *B* and *D* lines must be due to point defects rather than related to dislocations. The same behavior has been observed also in samples of the set DAT1.

(ii) Spectra referring to samples with different dislocation densities in the set DAT3 [Fig. 2(b)] show that the peak amplitude of line *C* scales with N_D, in contrast to the amplitudes of lines *B* and *D*, whereas the amplitude of line *A* increases, but with a different rate.

(iii) Furthermore, from the spectra in Figs. 2(a) and 2(b) it can be noted that, while peaks *A*, *B*, and *D* represent

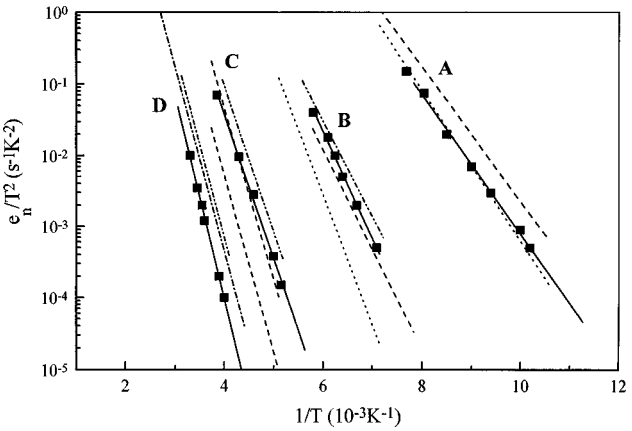

FIG. 1. Thermal emission rates (T^2 corrected) as a function of the inverse temperature for the DLTS peaks observed in the less deformed samples of the set DAT3 (■). Filling pulse height, $U_p = 0.3$ V; reverse bias, $U_r = 7$ V; filling pulse width, $t_p = 100$ μs. Also included are the data from Ref. 3 (dashed lines), Ref. 9 (dotted lines), and Ref. 10 (dash-dotted lines).

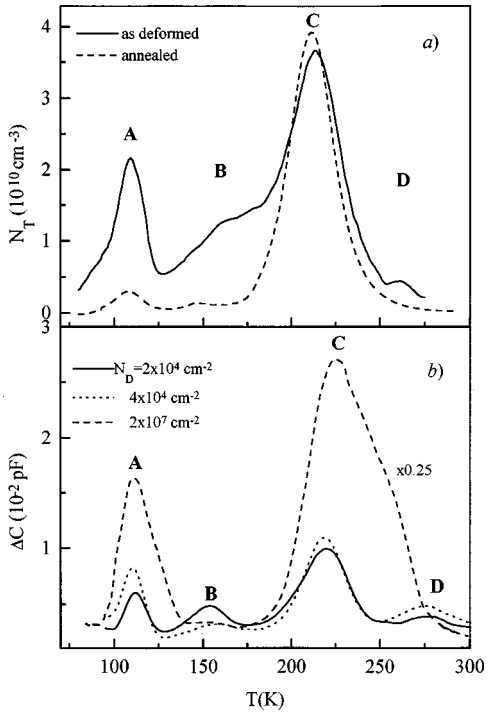

FIG. 2. (a) Deep-level transient spectroscopy spectra of a sample (dislocation density 10^4 cm^{-2}) of the set DAT3 before (solid line) and after (dashed line) the annealing procedure. ($e_n = 134$ s^{-1}, $U_p = 0.3$ V, $U_r = 7$ V, and $t_p = 100$ μs). (b) DLTS spectra of the samples with different dislocation densities of the set DAT3. $e_n = 134$ s^{-1}, $U_p = 0.3$ V, $U_r = 7$ V, and $t_p = 100$ μs.

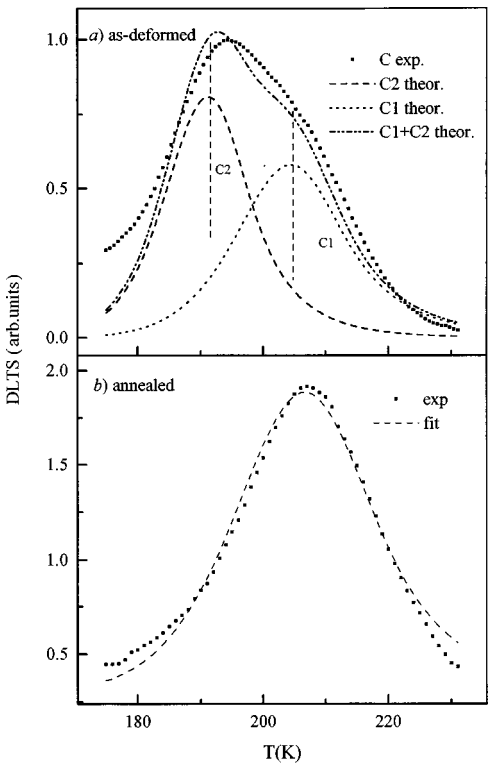

FIG. 3. Experimental spectra of the line C in the set DAT1: (a) in as-deformed samples line C is given by the sum of two contributions ($C1$ and $C2$) and (b) in annealed samples the C peak is obtained by the fitting with the model for broadened deep levels. $e_n = 57\ s^{-1}$, reverse bias, and filling pulses are the same as in Fig. 2. The values of the fitting parameters are reported in Table I.

''single-level peaks,'' i.e., they are not broadened, peak C is clearly broadened, as it will be shown in detail in the following.

From now on we will concentrate on the results referring to line C. Figure 3 shows the experimental C line in a typical DAT1 sample before and after annealing. This line consists of two different components $C1$ and $C2$ in the as-deformed samples, while it is a single, broad line in the annealed samples. The corresponding parameters are reported in Table I. In DAT3 the peak C remains almost unchanged [Fig. 2(a)] due to the partial annealing during the deformation. In the following we shall present the characteristics of the broad C line.

A. Capture kinetics

The capture mechanism of the trap C has been studied in the slightly deformed specimens of sets DAT1 and DAT3, where all the peaks are well separated. It is worth noting that the DLTS peak of trap C increases its amplitude as a function of the filling pulse width t_p, holding a nearly symmetric shape (Fig. 4), contrary to what has been observed by other authors.[5]

In the range of short filling pulses ($t_p < 10^{-6}$ s) the DLTS line amplitude ΔC_m of an ideal point defect depends on t_p according to an exponential law.[3] Thus, from the plot of ΔC_m vs t_p, the capture cross section σ_n can be evaluated. However, in plastically deformed materials it has been

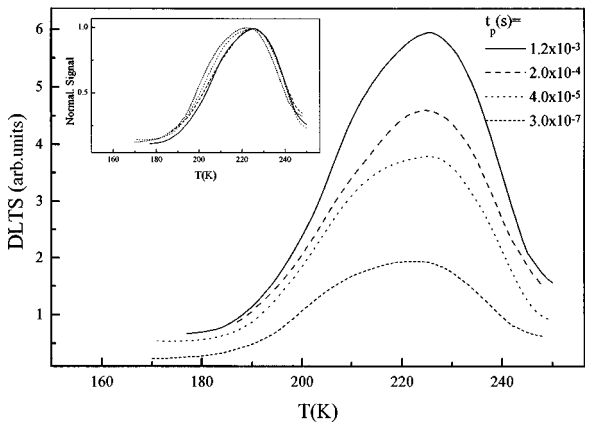

FIG. 4. Measured DLTS lines in a sample of the set DAT3 at different filling pulse widths. In the inset each spectrum has been normalized to its maximum value. The reverse bias is the same as in Fig. 2.

shown that ΔC_m linearly depends on $\ln(t_p)$.[10] This logarithmic capture mechanism has been modeled[10] by a defect whose potential barrier ϕ is time dependent through the equation

$$q\phi(t_p) + kT \ln \frac{n_T}{N_T} \approx kT\left[\ln(n\langle v_{\rm th}\rangle \sigma_n t_p) + \ln\left(\frac{n_T}{t_p \partial n_T/\partial t_p}\right)\right], \tag{3}$$

with N_T the whole trap density, n_T the density of traps filled by electrons, and n the free-electron density.

In the range of short t_p, the cross section σ_n of line C has been evaluated and reported in Table I for the DAT3 and DAT1 sets. In the range of long $t_p (10^{-6}\ \text{s} < t_p < 10^{-4}\ \text{s})$, n_T has been evaluated from ΔC_m and reported as a function of t_p in Fig. 5. It is to be noted that n_T shows a linear dependence on $\ln(t_p)$ up to 2×10^{-4} s. From these data and by using Eq. (3), the time-dependent potential barrier related to line C has been calculated and reported in Fig. 5. Similar behavior has already been observed for lines B and D,[10] but the capture kinetics of line C has never been studied up to now.

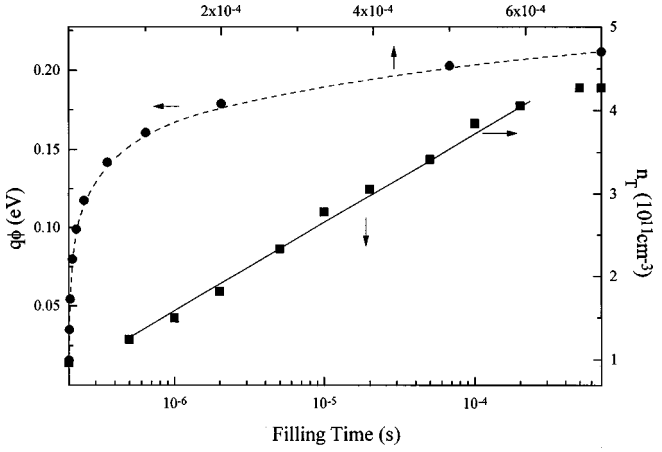

FIG. 5. Concentration of filled deep levels n_T, corrected for line broadening, and repulsive Coulomb potential $\phi(t_p)$, as a function of the filling time t_p for the C level. The straight line indicates the range where n_T is linear with $\ln(t_p)$.

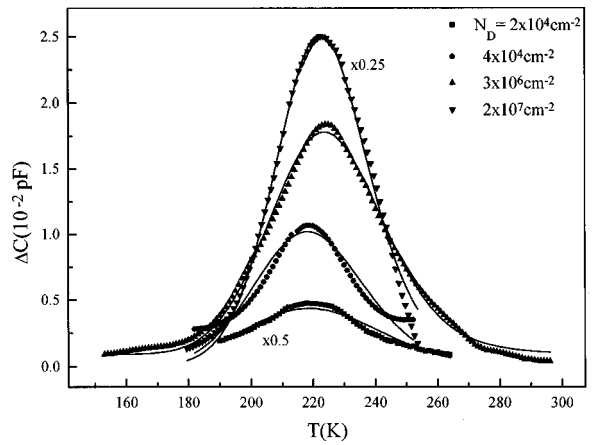

FIG. 6. Theoretical fit to the experimental spectra of the line C in samples with different dislocation densities of the DAT3 set. $e_n = 134\ s^{-1}$. Reverse bias and filling pulse are the same as in Fig. 2.

B. Broadening

As already stated, line C is a symmetrically broadened line. To describe this broadening effect we adopted the model developed by Omling, Samuelson, and Grimmeis,[11] reported in Sec. III, to fit the experimental DLTS spectra. This model successfully describes the symmetrical line broadening observed in almost all the spectra. Only in samples with high values of N_D [Fig. 2(b), dashed curve, $N_D = 2\times10^7\ cm^{-2}$] the C line becomes asymmetrical, due, in our opinion, to the overlapping with the D line. Consequently, to fit the C peak in the highly deformed samples, a deconvolution has been necessary to separate its contribution from the one of the D line.

An example of the best estimates of the parameters obtained from the fitting procedure are reported in Table I for the DAT3 and DAT1 sets. The fitting has been carried out simultaneously over five different spectra referring to five different emission rates in order to reduce the uncertainty of the estimated parameters. It is to be noted that, as already stated, peaks A, $C1$, and $C2$ are not broadened, while the fitting of peak C gives measurable FWHM values in each sample.

In Fig. 6 the theoretical fit to the experimental spectra of the C level in samples with different dislocation densities is reported. All the C peaks have been fitted simultaneously with the same value of activation enthalpy and prefactors but with different values of line amplitudes and FWHM's. The parameters obtained have been reported in Fig. 7 as a function of the dislocation density, i.e., in Fig. 7(a) the broadening parameter δ is plotted versus N_D, while in Fig. 7(b) the linear state density of line C, n_D, defined as $n_D = N_T(C)/N_D$, where $N_T(C)$ represents the concentration of line C, is plotted versus N_D. It is to be noted that both the parameters present the same decreasing trend versus N_D.

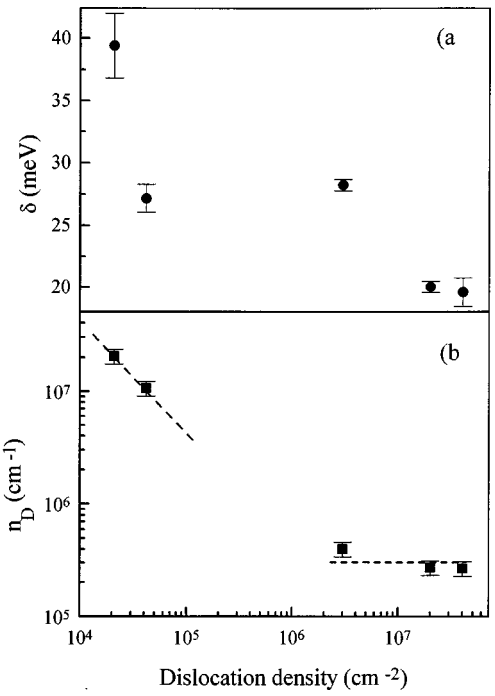

FIG. 7. (a) Broadening parameter δ of the line C plotted as a function of the dislocation density. (b) Linear state density of the line C, defined as $n_D = N_T(C)/N_D$, plotted vs the dislocation density N_D. The dashed lines are only a guide for the eye.

V. DISCUSSION

Extended defects interact with point defects and behave as segregation centers for impurities. It is therefore important to clarify whether or not the examined defects are ''clean'' to verify whether the observed deep levels are due to impurities or to intrinsic characteristics of the defects. As the reference samples did not show any traps, we can conclude that the observed deep levels must be induced by the deformation. If contamination had taken place, this would result in a concentration of impurities lower than the detectivity limit of the technique $(1-2)\times10^{10}$ traps/cm^3. Evidently, this definition of clean dislocation can only give the upper limit of possible contamination effects.

As already stated, we believe that the level most closely related to dislocations among the deformation-induced deep levels is line C. Several literature results agree with this conclusion.[1,4,12] Regarding the other levels, we have observed that B and D lines almost completely anneal out at 850 °C, while A line shows a higher thermal stability. Its contribution decreases after annealing [Fig. 2(a)], but clearly remains detectable. It increases with dislocation density, however, with a lower rate than line C. We also observed that trap A is inhomogeneously distributed in the crystal.[13] Notwithstanding its high thermal stability, we can exclude that traps A and C can be related to the same defect. As a matter of fact, the potential barrier associated with trap C induces a band bending of 0.23 eV. Trap A, if located close to trap C, is shifted above the Fermi level due to the band bending, becoming undetectable by DLTS. As we always detect both A and C levels, we can assess that they are not related to the same defect. Trap A could be thus identified with point-defect clusters related in some way to dislocation motion.

Main features of the trap C

We will now discuss the results referring to line C, in particular its reduction from a double line to a single broad line during annealing. In Fig. 8 the thermal emission rates

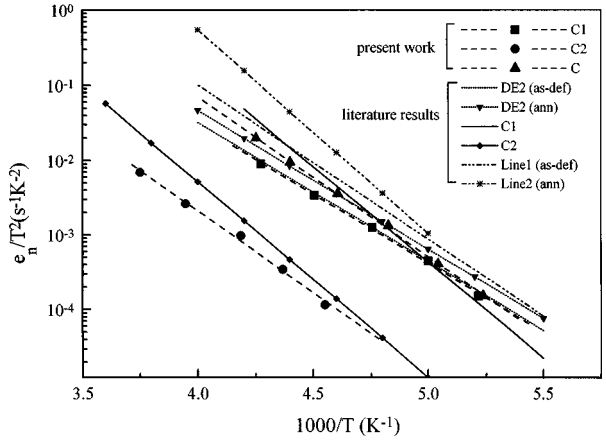

FIG. 8. Thermal emission rates ($-T^2$ corrected) of the levels $C1$ (■), $C2$ (●), and C (▲), referring to the present paper, are plotted as a function of the inverse temperature together with the literature results of Ref. 10 (DE2), Ref. 3 ($C1$ and $C2$), and Ref. 4 (lines 1 and 2).

($-T^2$ corrected) of levels $C1$, $C2$, and C are compared with literature data. Notwithstanding a large data scatter, two different groups of lines, here labeled $C1$ and $C2$, can be distinguished. Level C could be included in the $C1$ group, as confirmed also by the spectra of Fig. 3 and by the results of the fitting procedure shown in Table I. As the two levels $C1$ and $C2$ have very similar activation enthalpies but different prefactors, they have been attributed[3] to the same defect located in different surroundings of the crystal. According to this hypothesis, trap $C2$ could be related to point-defect clusters located close to the dislocations, while $C1$ should be due to the same defect cluster localized at the dislocations. Some of the defects responsible for $C2$ would disappear during annealing, while others would move toward the dislocations contributing to $C1$. This hypothesis would explain the disappearance of line $C2$ and the broadening of line C. Indeed, the resulting trap C corresponds to trap $C1$, but with larger prefactor (i.e., with larger capture cross section) and becomes broadened due to an increase in the crystal disorder in its surroundings.

The analysis of the capture kinetics of trap C, in particular the behavior of the DLTS peak C as a function of the filling pulse width t_p, can be explained in the framework of the model by Schroeter *et al.*[5] The authors classify many-electron defects states in bandlike or localized states, depending on the rate R_i at which the states reach internal equilibrium compared with the rates R_c and R_e at which they attain equilibrium with the valence and conduction bands. In particular, if $R_i \ll R_c, R_e$ the states are localized. The ''signature'' in DLTS analyses for localized states is the coincidence, after normalization, of the high-temperature side of DLTS spectra taken at different t_p's and the logarithmic filling pulse dependence of the DLTS line amplitude. As the capture kinetics of line C just fulfills these conditions, we ascribe C to localized states. Furthermore, its DLTS peak is symmetrically broadened, meaning that these states are likely symmetrically distributed in energy around a mean value E_a. Consequently, the model by Omling, Samuelson, and Grimmeis,[11] which neglects carrier exchange between the defect states and assumes a Gaussian distribution of energy states, applies.

To understand the broadening phenomenon, two different physical mechanisms can be recalled. Das, Singh, and Lang[15] used the broadening parameter to define weak and strong disorder in the crystal as follows: Weak disorder corresponds to $\delta/kT<1$ and $E_a/kT<0.1$, strong disorder to $\delta/kT>1$ and $E_a/kT>0.1$. By using this classification Kisielowski and Weber[8] state that plastically deformed silicon falls in the region between weak and strong disorder. The present results confirm this: δ/kT ranges from 1 to 2, while E_a/kT from 0.05 to 0.1, as reported also in Ref. 8. Thus crystal deformation induces disorder that contributes to the level broadening. A second mechanism to explain level broadening has been given by Morgan[16] and Stern.[17] From the analyses of fluctuations in the potential energy occurring among different sites of randomly distributed charge defects, they conclude that the broadening parameter δ must be an increasing function of the total ionized defect concentration N_a+N_d. In Fig. 7 the broadening parameter δ and the linear state density n_D of line C are reported as a function of the dislocation density N_D. By observing that both δ and n_D decrease versus N_D, a relation between δ and n_D can be assumed, in particular, δ is an increasing function of n_D, as predicted by the model reported in Refs. 16 and 17. From these findings it emerges that δ is not simply related to the structural characteristics of a specific defect, but it is rather related to the defect linear charge density, as well as to the lattice disorder.

VI. CONCLUSION

From deep-level transient spectroscopy analyses of plastically deformed, n-type silicon, the four traps A, B, C, and D usually found in this material have been detected. Particular attention has been paid to the DLTS line C, which dominates all the spectra. Due to its high thermal stability and because it scales well with the dislocation density, this line has been directly ascribed to dislocations. In particular its thermal stability, broadening, and capture kinetics have been studied in detail. The results can be summarized as follows: (i) It is a double line that simplifies after annealing, becoming a single, symmetrically broadened line; (ii) it is associated with localized states symmetrically spread in energy around a mean value E_a; (iii) it is associated with a time-dependent coulombic repulsive barrier; and (iv) it is associated with a broadening parameter δ, which is an increasing function of the dislocation linear state density. The line-broadening effect and the presence of a potential barrier for capture confirm that trap C must be related to a defect that experiences the dislocation strain field. Therefore, trap C is the most spatially localized at dislocations among all the deformation induced traps, while traps A, B, and D are mainly due to deformation-induced point defects not necessarily localized at dislocations. Trap A, which is quite stable after annealing and inhomogeneously distributed in the crystal, is not spatially localized at dislocations, even if it could be related in some way to dislocation motion. Our results confirm the identification of trap C with the electron-spin resonance (ESR) center Y (Ref. 18) because both these signals are composed by two contributions and they are the most thermally stable defects. The ESR center Si-Y has been

identified[3,18] with a threefold-coordinated vacancy in the core of screw dislocations. To summarize, dislocations contribute in different way to both traps *A* and *C*: Their movement contributes to the inhomogeneous distribution of the point defects responsible for trap *A* and they are preferential sites for vacancy agglomeration.

ACKNOWLEDGMENTS

M. Reiche of the Max-Planck-Institute für Mikrostrukturphysik, Halle, Germany, is gratefully acknowledged for HVEM measurements. The authors are also indebted to W. Schroeter for having provided the software for DLTS fitting.

[1] H. Alexander and H. Teichler, in *Materials Science and Technology, Electronic Structure and Properties of Semiconductors 4*, edited by W. Schroeter (VCH, New York, 1991), p. 249 and reference therein.

[2] V. V. Kveder, E. A. Steinmann, S. A. Shevchenko, and H. G. Grimmeiss, Phys. Rev. B **51**, 10 520 (1995).

[3] P. Omling, E. R. Weber, L. Montelius, H. Alexander, and J. Michel, Phys. Rev. B **32**, 6571 (1985).

[4] L. C. Kimerling and J. R. Patel, Appl. Phys. Lett. **34**, 73 (1979).

[5] W. Schroeter, J. Kronewitz, U. Gnauert, F. Riedel, and M. Seibt, Phys. Rev. B **52**, 13 726 (1995).

[6] K. Knobloch and H. Alexander, Mater. Sci. Eng. B **42**, 63 (1996).

[7] G. L. Miller, D. V. Lang, and L. C. Kimerling, Annu. Rev. Mater. Sci. **7**, 377 (1977).

[8] C. Kisielowski and E. R. Weber, Phys. Rev. B **44**, 1600 (1991).

[9] W. Szkielko, O. Breitenstein, and R. Pickenhein, Cryst. Res. Technol. **16**, 197 (1981).

[10] V. V. Kveder, Yu. A. Ossipyan, W. Schroeter, and G. Zoth,Phys. Status Solidi A **72**, 701 (1982).

[11] P. Omling, L. Samuelson, and H. G. Grimmeis, J. Appl. Phys. **54**, 5117 (1983).

[12] P. R. Wilshaw and T. S. Fell, in *Structure and Properties of Dislocations in Semiconductors*, edited by S. G. Roberts, D. B. Holt, and P. R. Wilshaw, IOP Conf. Proc. No. 104 (Institute of Physics and Physical Society, London, 1989), p. 83.

[13] D. Cavalcoli, A. Cavallini, and E. Gombia (unpublished).

[14] J. Kronewitz and W. Schroeter, Izv. Akad. Nauk SSSR, Ser. Fiz. **51**, 682 (1987) [Bull. Acad. Sci. USSR, Phys. Ser. **51**, 51 (1987)].

[15] A. Das, V. A. Singh, and D. V. Lang, Semicond. Sci. Technol. **3**, 1177 (1988).

[16] T. N. Morgan, Phys. Rev. **139**, A343 (1965).

[17] F. Stern, Phys. Rev. B **9**, 4597 (1974).

[18] C. Kisielowski, J. Palm, B. Bolling, and H. Alexander, Phys. Rev. B **44**, 1588 (1991).